DETECTION OF ASBESTOS CONTAINING MATERIAL IN POST-EARTHQUAKE BUILDING WASTE THROUGH HYPERSPECTRAL IMAGING AND MICRO-X-RAY FLUORESCENCE

Oriana Trotta [1],*, Giuseppe Bonifazi [1,2], Giuseppe Capobianco [1] and Silvia Serranti [1,2]

[1] Department of Chemical Engineering, Materials & Environment, Sapienza, University of Rome, Rome, Italy
[2] Research Center for Biophotonics, Sapienza, University of Rome, Latina, Italy

ABSTRACT

During an earthquake, a large amount of waste was generated, and many Asbestos-Containing Materials (ACM) were unintentionally destroyed. ACM is a mixture of cement matrix and asbestos fiber, widely used in construction materials, that causes serious diseases such as lung cancer, mesothelioma and asbestosis, as a consequence of inhalation of the asbestos fiber. In order to reuse and recycle Post-earthquake Building Waste (PBW) as secondary raw material, ACM must be separately collected and deposited from other wastes during the recycling process. The work aimed to develop a non-destructive, accurate and rapid method to detect ACM and recognize different types of PBW to obtain the best method to correctly identify and separate different types of material. The proposed approach is based on Hyperspectral Imaging (HSI) working in the short-wave infrared range (SWIR, 1000-2500 nm), followed by the implementation of a classification model based on hierarchical Partial Least Square Discriminant Analysis (hierarchical-PLS-DA). Micro-X-ray fluorescence (micro-XRF) analyses were carried out on the same samples in order to evaluate the reliability, robustness and analytical correctness of the proposed HSI approach. The results showed that the applied technology is a valid solution that can be implemented at the industrial level.

1. INTRODUCTION

Natural disasters create huge amounts of waste (Xiao et al., 2017). In 2016, an earthquake hit central Italy and produced about 3 million tons of waste, still clearly visible in terms of destruction in the epicentral area. Post-earthquake Building Waste (PBW) belong to the category of Construction and Demolition Waste (CDW) are mainly composed of materials like concrete, glass, asphalt, wood and also some hazardous materials like asbestos, still present in old buildings built before its ban in 1975 (Tabata et al., 2022). Asbestos is a fibrous mineral widely used in a variety of building materials due to its extraordinary tensile strength and resistance to heat and corrosion (Gualtieri, 2017; Paglietti et al., 2019). However, it causes serious diseases such as lung cancer, mesothelioma (Azuma et al., 2009) and asbestosis (EPA, 2020a). Many Asbestos-Containing Materials (ACM) are destroyed during an earthquake disaster, and there are risks that fine asbestos particles will spread in the air (Kim et al., 2015; Kim et al., 2020; Ishihara, 2012). In this perspective, after an earthquake, separation of ACM from PBW is required to remove this hazardous fraction,

thus allowing inert fractions to be recycled and reused as secondary raw material (Reinhart et al., 1999; Brown et al., 2011). Such an approach is of fundamental importance because it reduces the increase of landfilling, favoring the resilience of the affected areas and avoiding non-renewable raw materials exploitation.

PBW management is delicate asbestos-containing materials that are often not visible. The asbestos presence in building waste makes it dangerous for treatment, as currently, post-earthquake waste management is done manually by operators so that exposure can be harmful to their health.

A system based on Hyperspectral imaging (HSI) could be a valuable solution for recognizing and separating hazardous material from recycling products. Different studies have been carried out to perform asbestos fiber identification in ACM samples using the HSI techniques (Bonifazi et al., 2015, 2016, 2018, 2019; Serranti et al., 2019). In this study, instead, an object-based recognition of ACM materials was implemented in order to develop a classification model able to identify this material in respect of the main others usually constituting a PBW product (i.e., concrete,

tile, brick and stone). The classification method is based on the application of HSI working in the short-wave infrared region (SWIR: 1000−2500 nm) and micro-X-ray fluorescence (micro-XRF). More in detail, the acquired HSI data were first examined using Principal Component Analysis (PCA), and then a classification method based on hierarchical Partial Least Squares-Discriminant analysis (PLS-DA) was applied to detect ACM and PBW. The chemical maps obtained by micro-XRF were compared with the acquired hyperspectral images to validate the results obtained by optical sensing. The obtained results are very promising and representative of a variety of advantages, such as being non-destructive and accurate. Moreover, the proposed approach could be implemented at a recycling plant scale in order to develop an online strategies for sorting, with a minor exposure risk for workers.

2. MATERIALS AND METHODS

2.1 Analysed samples

The investigated samples are constituted of PBW and ACM fragments. The PBW samples, composed of tile, concrete, brick and stone coming from the collapsed building during the Amatrice (Italy) earthquake in 2016 and 2017, were collected from a stationary recycling plant (Cosmari Srl) located in the province of Macerata (Italy), where sorting and managing post-earthquake debris is performed. ACM samples, composed of a cement mortar and asbestos fibers mixture, were provided by National Institute for Insurance against Accidents at Work (INAIL) (Rome, Italy). Starting from these materials two sample data sets were built: one to calibrate and the other to validate the recognition/classification procedure. In both cases, four PBW samples and one ACM sample were selected (Figures 1a and 1b).

2.2 Hyperspectral imaging

Hyperspectral images were acquired using the SISUChema XL™ Chemical Imaging Workstation (Specim, Finland), equipped with an ImSpector™ N25E imaging spectrograph (Specim, Finland) working in the short-wave infrared range (SWIR, 1000-2500 nm). The analytical station is controlled by a PC unit equipped with specialised acquisition/pre-processing software (Chemadaq™) to handle the different

units and the sensing device constituting the platform and to perform the acquisition and the collection of spectra. Samples were acquired with a lens of 31 mm, and the spectral resolution was 6.3 nm. Spectral data were analyzed using the PLS Toolbox (Eigenvector Research, Inc., WA, USA) under Matlab® environment (The Mathworks, Inc., MA, USA).

2.3 Spectral data analysis

Hyperspectral data were pre-processed in order to highlight samples spectral differences and to reduce the impact of possible external sources of variability. Different combinations of the algorithm were applied, in particular:

- Smoothing (window: 21 pt): used for smoothing/noise reduction in order to avoid amplification of high-frequency noise during the derivation process, as it happens in the case of finite-difference derivation. It is an algorithm based on Savitzky−Golay routine (Rinnan et al., 2009),
- Multiplicative Scatter Correction (MSC) (median): works on imperfections (e.g., undesirable scatter effect) that will be removed from the data matrix prior to data modeling. MSC comprises two steps: estimating the correction coefficients (additive and multiplicative contributions) and correcting the recorded spectrum (Rinnan et al., 2009),
- Detrend: applied on spectra to remove the effects of baseline shift and curvilinearity (Otto, 1999; Rinnan et al., 2009),
- Mean Center (MC): it calculates the mean of each column of the matrix associated with the image and subtracts this from the column. It is useful for removing constant background contributions, which usually are not interesting for data variance interpretation (Rinnan et al., 2009).

2.4 Principal Component Analysis (PCA)

PCA was applied to explore the data, define classes and perform the calibration dataset. It is a valuable method that provides an overview of complex multivariate data. It was used to decompose the "processed" spectral data into several Principal Components (PCs), linear combinations of the original spectral data, embedding the spectral vari-
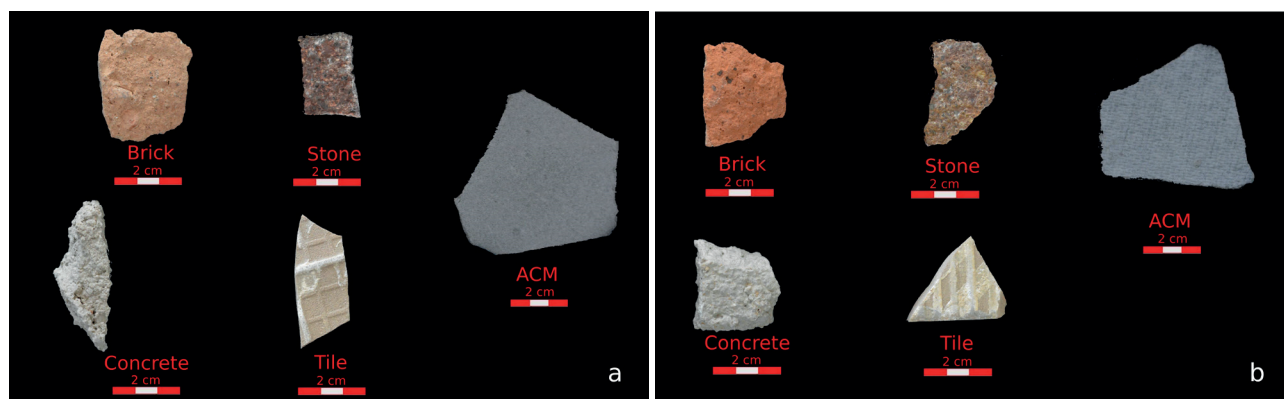

FIGURE 1: Digital images of the acquired samples: (a) calibration and (b) validation dataset.

ations of each collected spectral dataset (Bro et al., 2014; Wold et al., 1987; Cordella et al., 2012; Jolliffe et al., 2002).

2.5 Hierarchical PLS-DA Classification

The Partial Least Square-Discriminant Analysis (PLS-DA) method was applied in order to build a hierarchical model. It is a classification method used to find a model able to predict the known classes in an unknown image. Prior knowledge of the data was required. Starting from known samples, a specific function was built to predict the new unknown object in the HSI image, made of the same materials as the known classes (Ballabio et al., 2013; Barker et al., 2003).

The hierarchical model was used in order to preliminarily divide into subsets and then subdivide them into further subsets of the data until each subset contains a single object (Monakhova et al., 2016). The hierarchical classification procedure was based on 4 rules developed for classifying the five samples. In Figure 2, the developed dendrogram shows the hierarchical model built to classify the ACM and PBW.

The classification performances obtained by a hierarchical PLS-DA model were evaluated in terms of statistical parameters: Sensitivity and Specificity:

$$Sensitivity = \frac{True\ Positive}{(True\ Positive + False\ Negative)} \qquad (1)$$

$$Specificity = \frac{True\ Positive}{(True\ Positive + False\ Negative)} \qquad (2)$$

More in detail, Sensitivity estimates the model's ability to avoid false negatives, assessing the proportion of actual positives correctly identified, while Specificity allows the estimation of the model's ability to avoid false positives, that is, the proportion of negatives correctly identified. The more these values approach to 1, the better the model is.

2.6 Micro-X-ray Fluorescence analysis

Samples were analysed by micro-XRF to evaluate the chemical composition and element distribution. Micro-XRF analysis was performed by a Bruker Tornado M4 equipped with an Rh tube, operating at 50 kV, 200 µA, with a 25 µm spot obtained with poly-capillary optics. PBW samples mapping was carried out adopting an acquisition time of 10 ms/pixel and step size of 200 µm in vacuum conditions at 21 mBar. ACM samples mapping was performed adopting an acquisition time of 15 ms/pixel and step size of 100 µm in vacuum conditions at 20 mBar.

3. RESULTS AND DISCUSSION

3.1 Hyperspectral imaging

The sample's average reflectance spectra are shown in Figure 3. The raw spectra were preliminarily analyzed in order to detect and compare their characteristics. The absorption features, visible around 1400 nm and 1900 nm, are due to water molecules O-H stretching and H-O-H bending vibrations (Crowley et al., 2003). The absorptions evidenced in concrete spectra at 2350 nm identify calcite which is one of the ingredients of cement in the form of limestone and other forms of calcium carbonate (Goetz et al., 2009). The mean spectra of the ACM class show the vibrational spectroscopic effects in the wavelength ranges of 1380−1400 nm, indicating the presence in the samples of asbestos fibers (Bonifazi et al., 2019; Krówczyńska et al., 2017).

To improve separation between ACM and PBW materials, different pre-processing strategies were applied to reduce light scattering and emphasize the spectral differences, summarized in Table 1. Four different Rule were developed in order to build the classification model.

Rule 1 was adopted in order to perform a separation among the classes ACM+Stone+Brick and the classes Tile+Concrete. Rules 2 and 3 allowed for performing a two-step classification, preliminary detection Stone and further ACM and Brick. Finally, applying Rule 4 improved the separation between Tile and Concrete.

The results of the four Rules of the hierarchical PLS-DA classifier are presented and discussed in the following.

- **Rule 1**

The results of the pre-processed spectra and the corresponding PCA score are reported in Figure 4. The pre-pro-
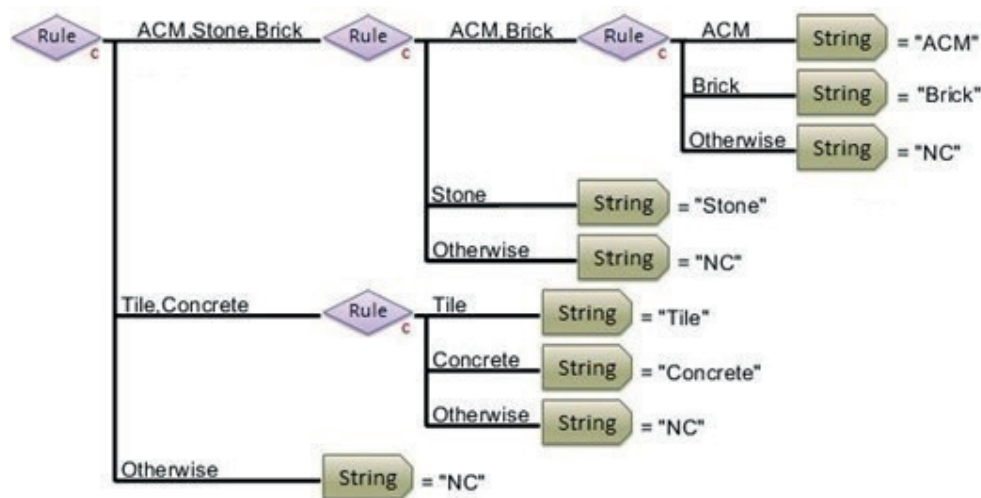

FIGURE 2: Dendrogram showing the hierarchical PLS-DA model built to classify the five different samples of ACM, Tile, Concrete, Brick and Stone.
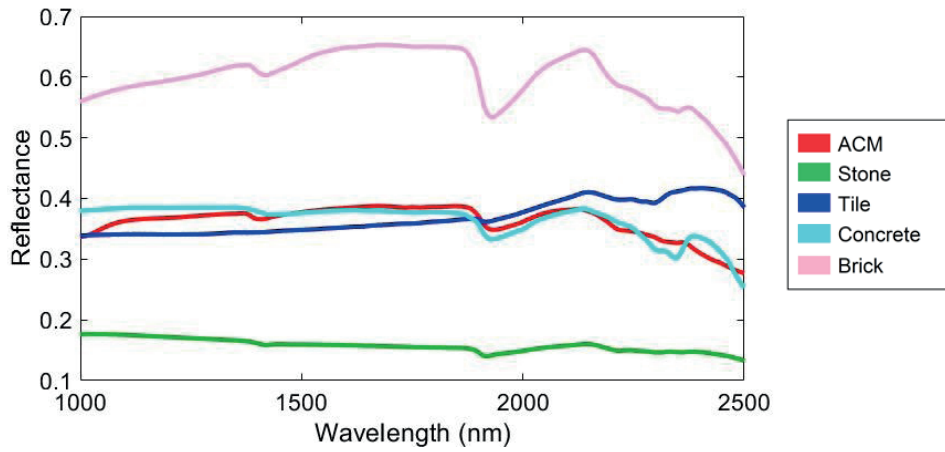
FIGURE 3: Average and reflectance spectra of the five classes of materials constituting the calibration dataset.

cessing combination selected for Rule 1 was Detrend and MC. The PCA results indicated that most of the variance was captured by the first two PCs, where PC1 and PC2 explained 70.49% and 14.55% of the variance, respectively. The spectral data of the five samples show a high variability due to the different types of materials.

- **Rule 2**

In Figure 5, the pre-processed spectra for Rule 2 were obtained through Smoothing and MC. The corresponding PCA indicates that most of the variance was captured by the first three PCs, where PC1 and PC3 explained 99.65% and 0.06% of the variance, respectively. As shown in the
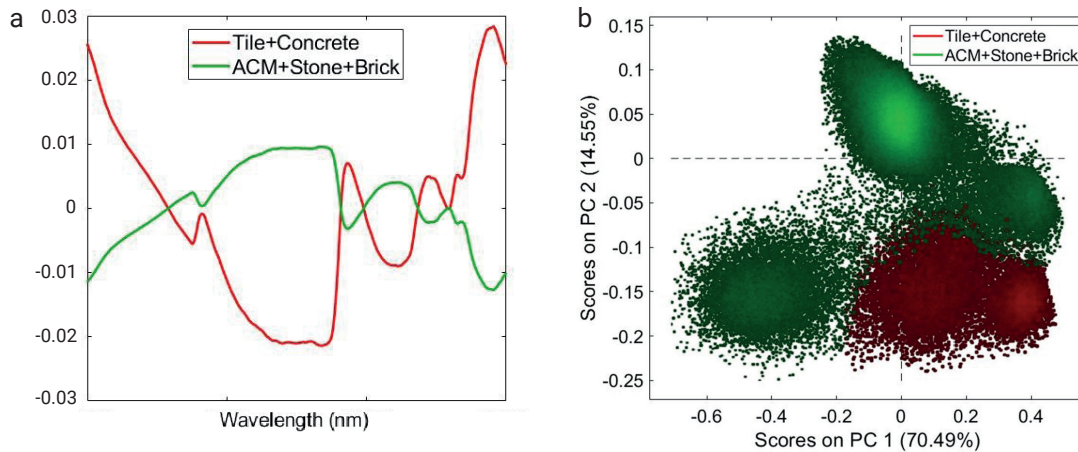

FIGURE 4: (a) Pre-processed (Detrend and MC) average reflectance spectra and (b) PCA score plot of PC1 and PC2 related to Tile+Concrete and ACM+Stone+Brick.
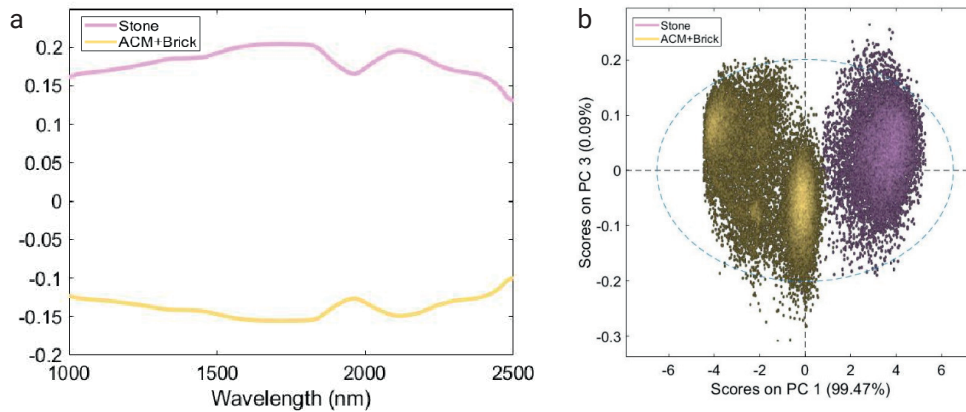

FIGURE 5: (a) Pre-processed (Smoothing and MC) average reflectance spectra and (b) PCA score plot of PC1 and PC3 related to ACM+Brick and Stone.

Rule	Pre-processing	Classification Output
1	Detrend	Tile+Concrete
	Mean Center	ACM+Stone+Brick
2	Smoothing (window: 21 pt)	ACM+Brick
	Mean Center	Stone
3	Multiplicative Scatter Correction (MSC) (median)	ACM
	Detrend Smoothing (window:15 pt)	Brick
	Mean Center	
4	Multiplicative Scatter Correction (MSC) (median)	Tile
	Detrend	Concrete
	Mean Center	

PCA score plot, ACM+ Brick and Stone were clustered into two groups.

• **Rule 3**

Rule 3 was developed to evaluate the spectral difference between ACM and Brick. In Figure 6, the results show the pre-processed spectra and the corresponding PCA score. The pre-processing selected were MSC, Detrend, Smooth-

ing and MC. PC1 and PC3 explained 50.39% and 27.53% of the variance, respectively, and the score plot shows a good separation between ACM and Brick.

• **Rule 4**

Finally, Rule 4 was obtained by the combination of the pre-processing MSC, Detrend and MC. In Figure 7, the results of the pre-processed average reflectance spectra and the corresponding PCA score plot. The first three PCs captured the variance, where PC1 and PC3 explained 85.02% and 2.63% of the variance, respectively. The PCA score plot shows a good separation between Tile and Concrete.

The classification model was then applied to the validation dataset and the obtained results were reported, in terms of a prediction map, in Figure 8. In Table 2, the classification results of objects, derived from the pixel based classification, presents no error. The results show a good prediction, but some errors occur because of the high variability and the complex morphology of the samples. The results, in terms of Sensitivity and Specificity in prediction phases, confirm the good quality of the model, with values ranging from 0.83 (i.e. tile) to 1.00 (i.e. brick) (Table 2).

The results achieved by the proposed HIS based approach are in agrrement with those obtained by other authors (Malinconico et al.2022, Frassy et al., 2014; Cilia et al., 2015).
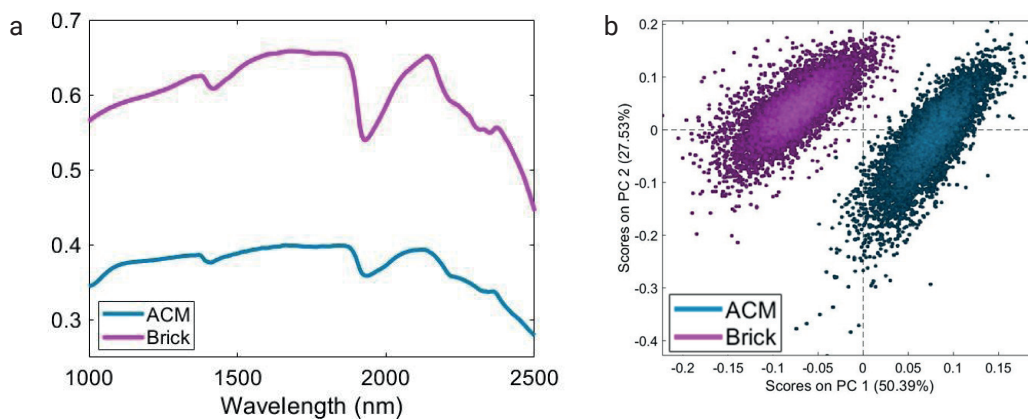

FIGURE 6: (a) Pre-processed (Detrend and MC) average reflectance spectra and (b) PCA score plot of PC1 and PC2 related to Tile+Concrete and ACM+Stone+Brick.
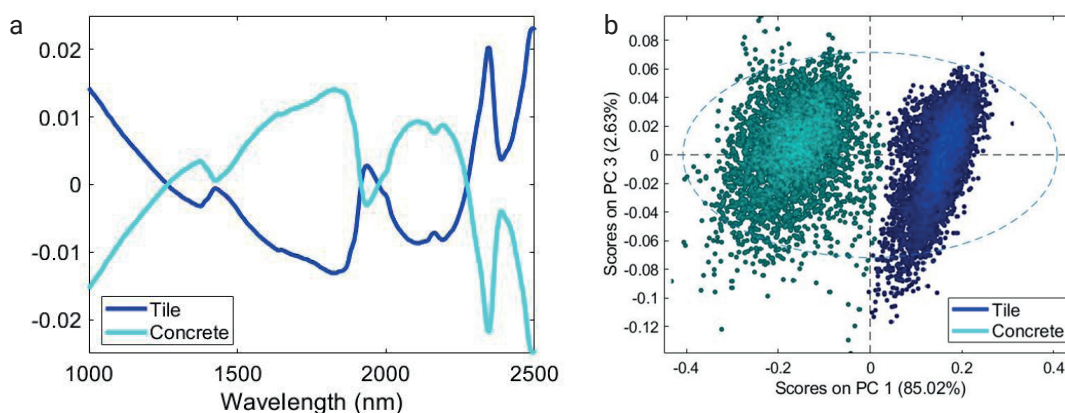

FIGURE 7: (a) Pre-processed (MSC, Detrend and MC) average reflectance spectra and (b) PCA score plot of PC1 and PC3 related to Tile and Concrete.
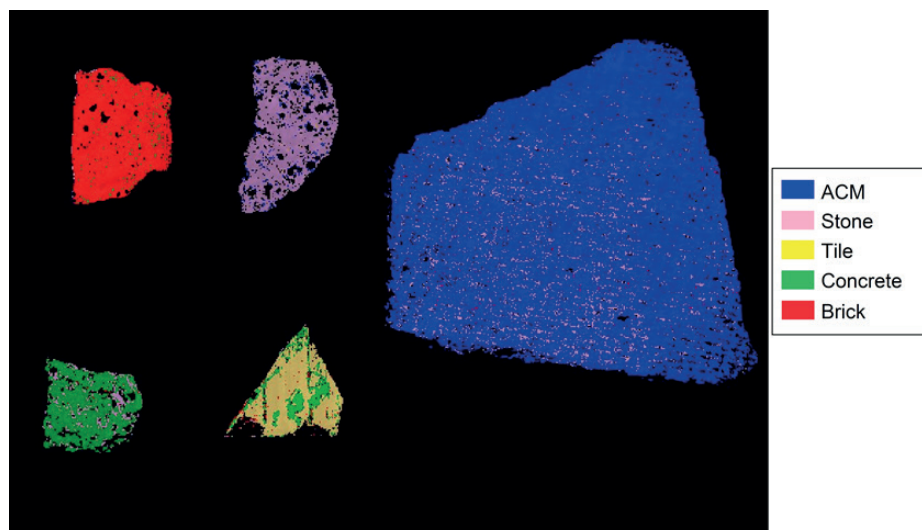
FIGURE 8: Results of the hierarchical PLS-DA classification model applied to the validation dataset.

3.2 Micro-X-ray Fluorescence

Micro-XRF maps were obtained on the same samples and compared with HSI prediction maps to evaluate their correctness. Micro-XRF results show differences in chemical composition and distribution between ACM and PBW samples (Figure 9). ACM sample shows different textural characteristics, in comparison to the other materials, due to the presence of asbestos fibers, identified by the detection of Fe and Mg, inside the cement mortar matrix, characterized by the presence of Ca and Al elements.

PBW samples are characterized, in agreement with the results obtained by HSI, by the presence of common elements but with different distribution and concentrations. Stones are mainly composed of different minerals containing Fe, Si and Al. Bricks show a matrix characterized by low porosity, with a high presence of Si and Fe. Concrete is mostly composed of Ca, which is also present as a contaminant on the surface of tile samples.

4. CONCLUSIONS

The present study was carried out to investigate the combined utilization of micro-XRF and HSI techniques to characterize asbestos-containing materials (ACM), a mixture of cement matrix and asbestos, and inert coming from buildings in a post-earthquake site. In order to reach this goal, a procedure based on the SWIR-HSI technique coupled with a chemometric approach was developed and a hierarchical PLS-DA model was built. Results clearly showed as the proposed method allowed to correctly identify ACM, tile, brick, concrete and stone materials in complete ac-cordance with HSI classification results and chemical element distributions verified by micro-XRF.

The advantage of the HSI technique, compared with micro-XRF, is that it represents a fast and easy to handle solution for post-earthquake building waste management. Moreover, this approach could be particularly useful to improve the detection of hazardous materials without human support and PBW recycling processes from post-earthquake sites. Future developments will be addressed to extend the classification to a different kind of ACM and increase the performance of selection at the recycling plant scale.

REFERENCES

Azuma, K., Uchiyama, I., Chiba, Y., Okumura, J., 2009. Mesothelioma risk and environmental exposure to asbestos: past and future trends in Japan. Int. J. Occup. Environ. Health. 15 (2), 166−172.

Ballabio, D., Consonni, V., 2013. Classification tools in chemistry. Part 1: Linear models. PLS-DA. Anal. Methods, 5, 3790−3798. https://doi.org/10.1039/C3AY40582F

Barker, M., Rayens, W., 2003. Partial Least Squares for Discrimination. J. Chemom., 17, 166−173.

Bonifazi, G., Capobianco, G., Serranti, S., 2015. Hyperspectral imaging applied to the identification and classification of asbestos fibers. Sensors.

Bonifazi, G., Capobianco, G., Serranti, S., 2016. A fast and reliable approach for asbestos recognition in complex matrices adopting an hyperspectral imaging based approach. In Proceedings of the 5th International Conference on Industrial & Hazardous Waste Management, Chania, Greece, 27−30.

TABLE 2: Classification performances, quantified in terms of Sensitivity and Specificity, resulting from the application of the hierarchical PLS-DA model.

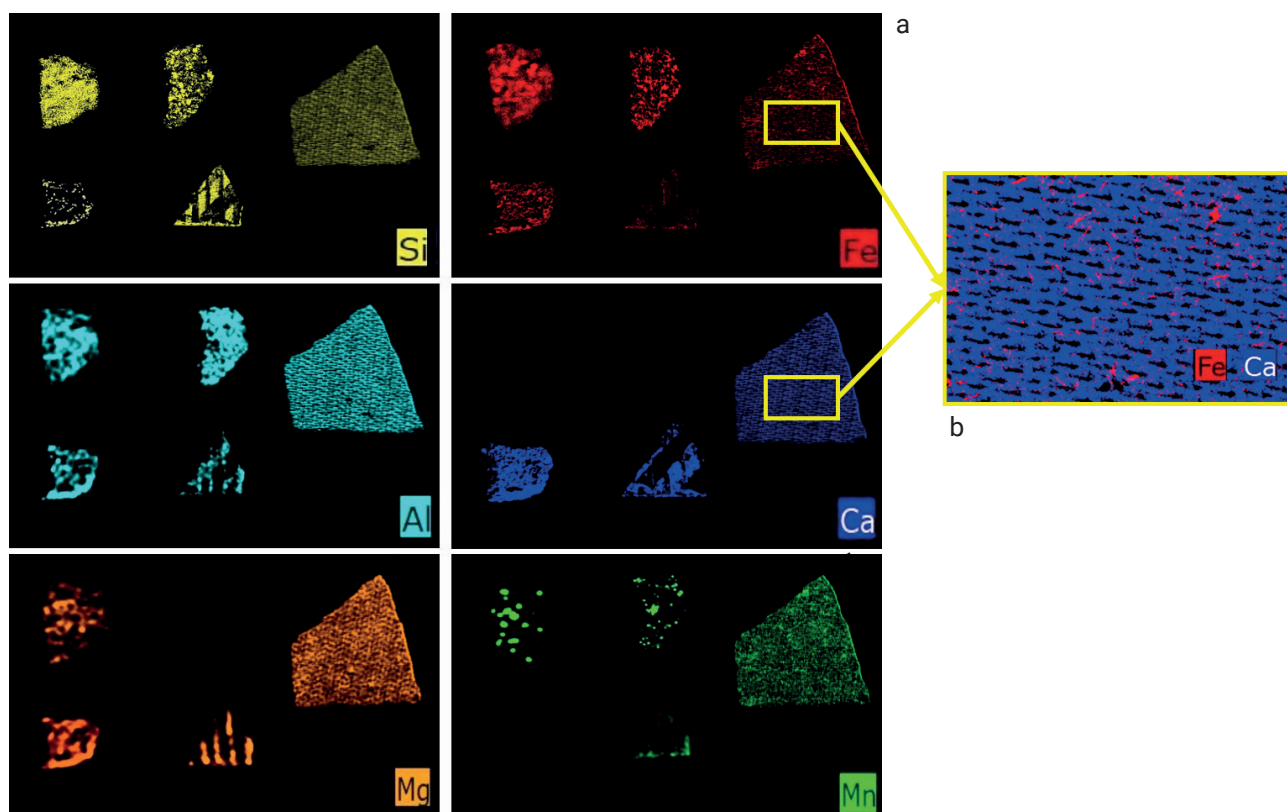|	Brick	Concrete	ACM	Stone	Tile
Sensitivity (Pred)	0.96	0.86	0.93	0.92	0.83
Specificity (Pred)	1.00	0.99	0.98	0.94	1.00

FIGURE 10: (a) Micro-XRF maps of validation dataset showing the distribution of principal elements and (b) ACM sample detail in which the distribution of Fe and Ca is shown, representing asbestos fibers and cement mortar matrix respectively.

Bonifazi, G., Capobianco, G., Serranti, S., 2018. Asbestos containing materials detection and classification by the use of hyperspectral imaging. J. Hazard. Mater. https://doi.org/10.1016/j.jhazmat.2017.11.056

Bonifazi, G., Capobianco, G., Serranti, S., 2019. Hyperspectral Imaging and Hierarchical PLS-DA Applied to Asbestos Recognition in Construction and Demolition Waste. Appl. Sci., 9, 4587. https://doi.org/10.3390/app9214587.

Bro, R., Smilde, A.K., 2014. Principal Component Analysis. Anal. Methods, 6, 2812–2831.

Brown, C., Milke, M., Seville, E., 2011. Disaster waste management: A review article. Waste Manag., 31, 6.

Cilia, C., Panigada, C., Rossini, M., Candiani, G., Pepe, M., Colombo, R., 2015. Mapping of asbestos cement roofs and their weathering status using hyperspectral aerial images, ISPRS Int. J. Geo-Inf. 4, 928–941.

Cordella, C.B.Y., 2012. PCA: The Basic Building Block of Chemometrics. Analytical Chemistry, Ira S. Krull, Intech Open.

Crowley, J.K., Williams, D.E., Hammarstrom, J.M., Piatak, N., Chou, I.M., Mars, J.C., 2003. Spectral reflectance properties (0.4-2.5 lm) of secondary Fe-oxide, Fehydroxide, and Fesulphate-hydrate minerals associated with sulphide-bearing mine wastes. Geochemistry: Exploration, Environment, Analysis, 3, 219–228.

EPA, USA, 2020a. EPA actions to protect the public from exposure to asbestos. 1–9, related issues in it. https://www.epa.gov/asbestos/epa-actions-protect-publicexposure-asbestos (accessed 27/01/22).

Frassy, F., Candiani, G., Rusmini, M., Maianti, P., Marchesi, A., Nodari, F.R., Via, G.D., Albonico, C., Gianinetto, M., 2014. Mapping asbestos-cement roofing with hyperspectral remote sensing over a large mountain region of the Italian western alps. Sensors 14, 15900–15913.

Goetz, A.F.H., Curtiss, B., Shiley, D.A., 2009. Rapid gangue mineral concentration measurement over conveyors by NIR reflectance spectroscopy. Minerals Engineering, 22, 490–499.

Gualtieri, A.F., 2017. Mineral Fibres: Crystal Chemistry, Chemical-Physical Properties, Biological Interaction and Toxicity. Eur. Mineral. Union Notes Mineral., 18, 7–9.

Ishihara, K., 2012. Revival from Earthquake Disaster and Asbestos Problems. J. of Policy Science, 6, 113-119.

Jolliffe, I.Y., 2002. Principal Component Analysis. 2nd Edition, Springer Series in Statistics. Berlin-HeidelbergNew York.

Kim, Y. C., Hong, W. H., & Zhang, Y. L., 2015. Development of a model to calculate asbestos fiber from damaged asbestos slates depending on the degree of damage. Journal of Cleaner Production, 86, 88-97.

Kim, Y. C., Zhang, Y. L., Park, W. J., Cha, G. W., & Hong, W. H.. 2020. Quantifying asbestos fibers in post-disaster situations: Preventive strategies for damage control. International Journal of Disaster Risk Reduction, 48, 101563.

Krówczyńska, M., Wilk, P., Pabjanek, E., Kycko, M., 2017. Hyperspectral discrimination of asbestos-cement roofing. Geomat. Environ. Eng., 11, 47–65.

Malinconico, S., Paglietti, F., Serranti, S., Bonifazi, G., & Lonigro, I., 2022. Asbestos in soil and water: a review of analytical techniques and methods. Journal of Hazardous Materials, 129083.

Monakhova, Y.B., Hohmann, M., Christoph, N., Wachter, H., Rutledge, D.N., 2016. Rutledge Improved classification of fused data: Synergetic effect of partial least squares discriminant analysis (PLS-DA) and common components and specific weights analysis (CCSWA) combination as applied to tomato profiles (NMR, IR and IRMS). Chemom. Intell. Lab. Syst., 156, 1–6.

Otto, M., 1999. Chemometrics, Statistics and Computer Application in Analytical Chemistry Wiley-VCH, New York.

Paglietti, F., Malinconico, S., Conestabile della Staffa, B., Bellagamba, S., De Simone, P., 2016. Classification and management of asbestos-containing waste: European legislation and the Italian experience, Waste Management, 50, 130-150, https://doi.org/10.1016/j.wasman.2016.02.014.

Reinhart, D., McCreanor, P., 1999. Disaster debris management–planning tools. US Environ. Prot. Agency Reg. IV, 4, 1–31.

Rinnan, Å., Nørgaard, L., van den Berg, F., Thygesen, J., Bro, R., Engelsen, S.B., 2009. Chapter 2 – data pre-processing. Infrared Spectrosc. Food Qual. Anal. Control, 29-50. https://doi.org/10.1016/B978-0-12-374136-3.00002-X

Rinnan, Å., van den Berg, F., Engelsen, S.B., 2009. Review of the Most Common Pre-Processing Techniques for near-Infrared Spectra. TrAC Trends Anal. Chem., 28, 1201–1222.

Serranti, S., Bonifazi, G., Capobianco, G., Malinconico, S., and Paglietti, F., 2019. Hyperspectral imaging applied to asbestos containing materials detection: specimen preparation and handling, Proc. SPIE 11007, Advanced Environmental, Chemical, and Biological Sensing Technologies XV, 110070S; https://doi.org/10.1117/12.2517070

Tabata, M., Fukuyama, M., Yada, M., Toshimitsu, F., 2022. On-site detection of asbestos at the surface of building materials wasted at disaster sites by staining, Waste Management, 138, 180-188, https://doi.org/10.1016/j.wasman.2021.11.039

Wold, S., Esbensen, K., Geladi, P., 1987. Principal component analysis. Chemom. Intell. Lab. Syst., 2, 37–52.

Xiao, J., Xie, H., Zhang, C., 2017. Investigation on building waste and reclaim in Wenchuan earthquake disaster area. Resour Conserv. Recycl. 61, 109–117. https://doi.org/10.1016/j.resconrec.2012.01.012.